



Polyphenol-based targeted therapy for oral submucous fibrosis

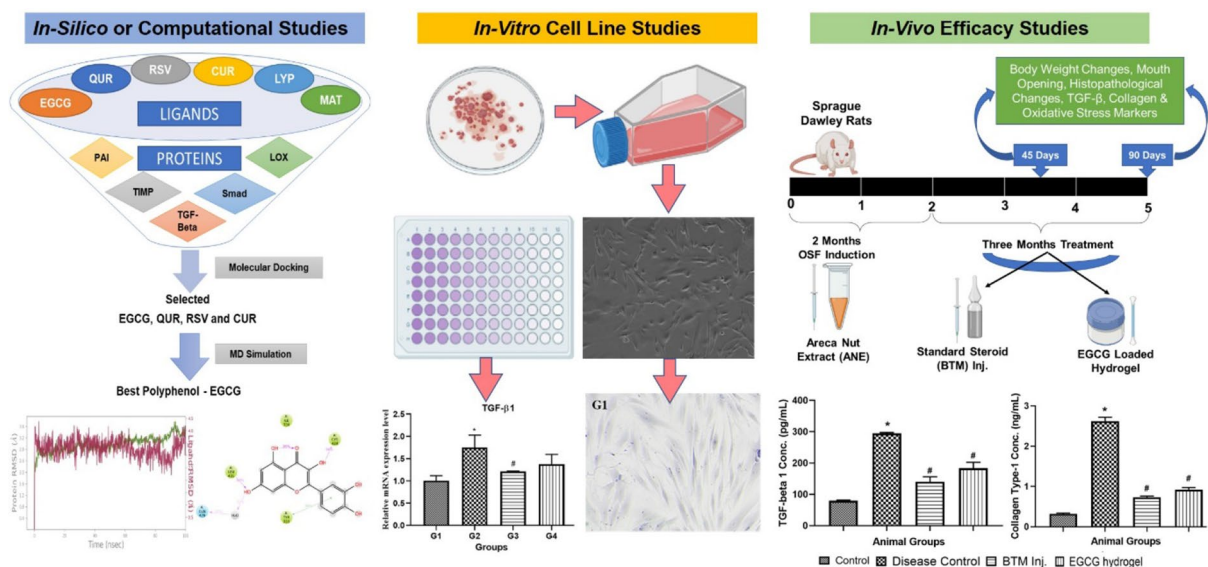
Chetan Hasmukh Mehta¹ · Shivangi Paliwal² · Manjunatha S. Muttigi² · Raviraja N. Seetharam² · Aleevoor Srinivas Bharath Prasad³ · Yogendra Nayak⁴ · Shruthi Acharya⁵ · Usha Yogendra Nayak¹

Received: 7 November 2022 / Accepted: 26 March 2023 / Published online: 27 April 2023
© The Author(s) 2023

Abstract

Oral submucous fibrosis (OSF) is a chronic, progressive, and precancerous condition mainly caused by chewing areca nut. Currently, OSF therapy includes intralesional injection of corticosteroids with limited therapeutic success in disease management. Therefore, a combined approach of *in silico*, *in vitro* and *in vivo* drug development can be helpful. Polyphenols are relatively safer than other synthetic counterparts. We used selected polyphenols to shortlist the most suitable compound by *in silico* tools. Based on the *in silico* results, epigallocatechin-3-gallate (EGCG), quercetin (QUR), resveratrol, and curcumin had higher affinity and stability with the selected protein targets, transforming growth factor beta-1 (TGF- β 1), and lysyl oxidase (LOX). The efficacy of selected polyphenols was studied in primary buccal mucosal fibroblasts followed by *in vivo* areca nut extract induced rat OSF model. In *in vitro* studies, the induced fibroblast cells were treated with EGCG and QUR. EGCG was safer at higher concentrations and more efficient in reducing TGF- β 1, collagen type-1A2 and type-3A1 mRNA expression than QUR. *In vivo* studies confirmed that the EGCG hydrogel was efficient in improving the disease conditions compared to the standard treatment betamethasone injection with significant reduction in TGF- β 1 and collagen concentrations with increase in mouth opening. EGCG can be considered as a potential, safer and efficient phyto-molecule for OSF therapy and its mucoadhesive topical formulation help in the improvement of patient compliance without any side effects.

Graphical abstract



Highlights

- Potential polyphenols were shortlisted to treat oral submucous fibrosis (OSF) using in silico tools
- Epigallocatechin 3-gallate (EGCG) significantly reduced TGF- β 1 and collagen both in vitro and in vivo
- EGCG hydrogel enhanced antioxidant defense, modulated inflammation by reducing TGF- β 1 and improved mouth opening in OSF rat model.

Keywords Oral submucous fibrosis · Polyphenols · Epigallocatechin 3-gallate · Quercetin · Transforming growth factor beta-1 · Collagen · Fibroblasts · OSF rat model

Introduction

Oral submucous fibrosis (OSF) is a chronic and inflammatory progressive scarring disease caused by chewing areca nut, betel quid, and gutka, resulting in the accumulation of connective tissue in lamina propria (Ray et al. 2019; Akshayak and Senthil Murugan 2021). Although this condition was observed earlier in South Asian countries, it has slowly crept into Europe and North America (Devarajan and Somasundaram 2019). It also results in serious morbidity among affected individuals. Multiple factors contribute to the disease progressions, such as defective collagen homeostasis, genetic susceptibility and immunity (Sharma et al. 2017). Arecoline is the main etiological factor responsible for OSF progression by activation of transforming growth factor-beta (TGF- β) signalling pathway. In turn, TGF- β activates other proteins, such as small mothers, against the decapentaplegic (Smad) protein, lysyl oxidase (LOX), and reactive oxygen species (ROS). These are responsible for collagen overproduction and reduction in collagen degradation by stimulating tissue inhibitors of the matrix metalloproteinase (TIMP) and plasminogen activator inhibitor (PAI) (Kondaiah et al. 2019). Out of these proteins, TGF- β 1 and LOX are the validated drug targets for inhibiting TGF- β signalling pathway (Sharma et al. 2018).

Currently, a blend of strategies have been adopted for the treatment of OSF namely habit control, drugs, surgical, physiotherapy, laser treatment and nutritional interventions. The drugs include corticosteroids (dexamethasone/betamethasone/ hydrocortisone/ triamcinolone) alone or in combination with hyaluronidase and lycopene (LYP). The intralesional injection of corticosteroids suppresses TGF- β 1 and forms the mainstay in the treatment of OSF (Shih et al. 2019). Nonetheless, none of the therapies have resulted in the successful treatment of OSF apart from rendering symptomatic relief to patients (Gopinath et al. 2022). The standard treatment, corticosteroid injection reported side effects with higher chances of infection at the site of injection and

systemic side effects such as adrenal insufficiency, edema, osteonecrosis, osteoporosis, myopathies and central serous chorioretinopathy, Hence, there is a need to identify an effective strategy for the treatment of OSF, which can be an alternative to the currently available treatment and provide symptomatic relief. The literature states that non-steroidal anti-inflammatory drugs (NSAIDs), angiotensin-converting enzyme (ACE) inhibitors, and angiotensin receptor blockers (ARB) can be used to treat OSF (Wollina et al. 2015) but there efficacy is not yet proved in the treatment of OSF. As per one research studies, It was observed that among various selected patients for study, 05 (45.46%) and 06 (54.54%) patients showed mild and severe fibrosis when they were using the NSAIDs for about 6 months (Hira et al. 2016). Therefore the drugs having all the activities such as anti-fibrotic, anti-inflammatory and oxygen radical scavenging properties are more beneficial for the effective treatment of OSF (Xia and Li 2019; Chandran et al. 2022). The use of plant-based active moieties shows significant benefits with required safety. Medicinal plants such as cruciferous vegetables, garlic, andrographolide are explored for the treatment of different disorders such as cancer (Akkol et al. 2020; Ağagündüz et al. 2022; Mitra et al. 2022), psychiatric and neurological disorders (Vieira et al. 2020; Akkol et al. 2020; Farooq et al. 2021), thrombotic, inflammatory and nociceptive conditions (Khan et al. 2020; Uddin Chy et al. 2021), fibromyalgia (Ferrarini et al. 2022), hyperglycemic and diabetic conditions (Mechchate et al. 2021; Haque et al. 2022), antidepressant, antidiarrheal and anxiolytic activity (Hosain et al. 2021; Jahan et al. 2022) and many other chronic disorders (Iqbal et al. 2020).

The naturally occurring polyphenols, lycopene (LYP) and curcumin (CUR) were attempted as therapeutic agents for the treatment of OSF. Saran et al. proved that polyphenol LYP is better than CUR in the management of OSF (Saran et al. 2018). Polyphenols such as epigallocatechin 3-gallate (EGCG) (Hsieh et al. 2017), quercetin (QUR) (Li et al. 2018), matrine (MAT) (Liu et al. 2018) and resveratrol (RSV) (Zeng et al. 2018) have been reported to possess anti-fibrotic, anti-inflammatory and oxygen radical scavenging properties. Based on the literature evidence, in the present study, an attempt was made to screen the potential polyphenols that can be used to treat OSF. Thus, in the present work, in silico studies such as molecular docking and molecular

dynamic (MD) simulation were performed to analyse the molecular stability of ligands such as EGCG, CUR, RSV, QUR, LYP and MAT towards the target proteins of OSF such as TGF- β 1 and LOX. The efficacy of the best polyphenols was examined using in vitro cell line studies in primary buccal mucosal fibroblasts cells and areca nut extract (ANE) induced rat OSF model.

Materials and methods

Materials

Epigallocatechin 3-gallate and quercetin were purchased from TCI chemical, India. Arecoline hydrobromide, ferric chloride (FeCl_3), 2,4,6-tris(2-pyridyl)-s-triazine (TPTZ), naphthyl ethylenediamine dihydrochloride, 2,2-diphenyl-1-picryl-hydrazyl-hydrate (DPPH), Biebrich scarlet and Ponceau BS were purchased from Sigma-Aldrich-Merck, India. (3-(4,5-dimethylthiazol-2-Y1)-2,5-diphenyltetrazolium bromide), DTNB (5,5-dithio-bis-(2-nitrobenzoic acid)) also known as Elman's Reagent, dimethyl sulfoxide (DMSO), 2-thiobarbituric acid, adrenaline bitartrate, and sodium deoxycholate were purchased from the HiMedia, India. Betamethasone injection I.P. (Betamsole, manufactured by Laborate Pharmaceuticals India Ltd) was procured from the Kasturba Hospital Pharmacy, Manipal, India. Penicillin-streptomycin (PenStrep, 5000 U/mL), GlutaMAX Supplement, Dulbecco's Modified Eagle Medium low-glucose (DMEM-Lg), Dulbecco's phosphate-buffered saline (DPBS), and fetal bovine serum (FBS) was purchased from Gibco, Thermo Fisher Scientific, India. Weigert's haematoxylin solution, acid fuchsin, phosphotungstic acid hydrate extrapure, phosphomolybdic acid extrapure, aniline blue (water soluble, methyl blue), sulphanilamide, molecular biology grade of ethanol, chloroform and isopropanol were purchased from the Sisco Research Laboratories Pvt. Ltd., India. Glacial acetic acid and ethanol were purchased from Merck Life Sciences Pvt. Ltd., India. RNAiso Plus, Prime Script RT reagent K (Perfect) and SYBR Premix Ex Taq (Tli RNaseH Plus) were purchased from DSS Takara Bio India Pvt. Ltd. Areca nuts extract was purchased from Vital Herbs, India. Rat transforming growth factor-beta 1 (rat TGF- β 1) and rat collagen types 1 alpha 1 (rat COL1a1) enzyme-linked immunosorbent assay (ELISA) kits were purchased from Maxome Labsciences, India, and Elabscience, India, respectively. Sodium dihydrogen phosphate (NaH_2PO_4), disodium hydrogen phosphate, sodium carbonate (Na_2CO_3), potassium dihydrogen orthophosphate, disodium hydrogen orthophosphate, potassium chloride,

ortho-phosphoric acid, trichloroacetic acid (TCA), butylated hydroxytoluene (BHT), hydrochloric acid (HCl), potassium dihydrogen orthophosphate (KH_2PO_4), disodium phosphate (Na_2HPO_4), hydrogen peroxide (H_2O_2), and sodium chloride were purchased from the S D Fine Chemicals, India. All analytical grade reagents were used.

Methods

Molecular modelling

The molecular modelling platform Maestro (Schrödinger, LLC, NY, 2019) was used for performing molecular docking, followed by MD simulation studies using a workstation with Intel® Xeon® Gold 6130 Processor with 2.1 Ghz 16C/32 T 22 M cache having Nvidia Quadro P5000 graphical processing unit cards and Ubuntu 18.04.3 LTS operating system.

Preparation of ligands

The ligands, namely EGCG, QUR, CUR, LYP, MAT, and RSV, were taken from PubChem and drawn using a 2D sketcher in Maestro Module and converted to the 3D structure. The structures of all polyphenols were optimized using the 'LigPrep' tool of Schrödinger, to obtain the geometry optimized with the lowest energy at neutral pH 7.0 ± 0.0 .

Protein preparation

The crystal structures of proteins were selected after careful screening based on their resolution. The proteins LOX (PDB ID: 5ZE3, Resolution: 2.40 Å), and TGF- β 1 (PDB ID: 4X2G, Resolution: 1.51 Å) were downloaded from the 'Protein Data Bank' (PDB) (<https://www.rcsb.org/>). The structures were processed with 'Protein Preparation Wizard' (PPW) (Madhavi Sastry et al. 2013), wherein the missing hydrogen atoms, amino acid residues, and missing side chains were added. The proper ionization state for protein residues was generated, the water molecules beyond 5 Å were removed, and H-bond (HB) network was generated. Finally, the protein structure was minimized using the OPLS3 force field (Harder et al. 2016). A homology model was generated using 'Prime' module for the proteins for which the crystal structure was not reported (Jacobson et al. 2004). Using the BLAST tool, the protein structure with the highest homology to the query protein was selected as the template protein. Using the ClustalW, the amino acid of the query protein was aligned with the template protein. The structural model was built using the default settings in Prime. The 'SiteMap' tool (Halgren 2007, 2009) was used to identify the druggable, ligand-binding site for the protein.

Molecular docking studies

Molecular docking was performed using the ‘Glide’ module in Schrödinger to examine the molecular affinity of ligands towards the selected proteins (Friesner et al. 2004, 2006; Halgren et al. 2004). Using the Glide grid, the binding site was defined, and the ligands were docked with standard precision (SP) mode (Friesner et al. 2004, 2006).

MD simulations studies

The MD simulation study was performed to assess the stability between the protein and ligand using the ‘Desmond’ module in Schrödinger (Bowers et al. 2006). Initially, a solvated complex system was prepared using TIP3P water model, the system was neutralized by adding counter ions, and the iso-osmotic condition was maintained during simulation by adding 0.15 M NaCl using the ‘System Builder’ module. The solvated system was minimized using the 2000 maximum iterations and 1.0 (kcal/mol/Å) convergence threshold. The minimized system was used for running the MD simulation. The MD simulation was performed via NPT ensemble for 100 ns at 1.01 bar pressure and 300 K temperature using Nose–Hoover chain thermostat (1 ns) and Martyna–Tobias–Klein barostat (2 ns). During the simulation, 1000 structures were saved to the trajectory. The MD simulation trajectory was analyzed using the simulation interaction diagram in Desmond, and the polyphenols are graded for their best binding, and stable root mean square deviation (RMSDs).

In vitro cytotoxicity and efficacy study

The in vitro cytotoxicity, the efficacy of EGCG and QUR were analysed using primary buccal mucosal fibroblasts cells.

Buccal mucosal fibroblast culture

Human buccal mucosal samples were collected after having informed consent from healthy volunteers according to the approved protocol by the Institutional Ethical Committee (IEC), Kasturba Medical College, MAHE, Manipal (#285/2021). Briefly, 4 mm biopsy specimen from third molar extraction site was taken from healthy volunteers (normal subjects with no habits of smoking and betel quid chewing of age between 18 and 32 years) using a biopsy punch and transported into a sterile medium containing 1%

penicillin–streptomycin (Pen–Strep) solution (10,000 units/mL of penicillin and 10,000 µg/mL of streptomycin).

Primary tissue culture

The collected human buccal mucosal samples were washed three times with DPBS containing 1% PenStrep. Further, tissue samples were minced into small pieces using a sterile blade and placed on the tissue culture plate in a medium containing DMEM-Lg, 10% FBS, 1% glutaMAX and 0.5% PenStrep. Tissue culture plates were then incubated at 37 °C under 95% O₂ and 5% CO₂ air atmosphere (ESCO CelCulture CO₂ Bioincubator, USA). The tissue culture plates were screened under an inverted microscope (Thermo Invitrogen EVOS M5000 Fluorescence inverted microscope, USA), and a culture medium was added every alternative day until explant monolayer cultures were 70 to 80% confluent. The fibroblasts were passaged using trypsin–EDTA and expanded in T75 flasks. Fibroblasts cryopreserved at passage 2 were used for all experiments (Adtani et al. 2018; Banerjee et al. 2021).

In vitro cytotoxicity studies

The effect of EGCG and QUR on viability and proliferation of primary buccal mucosal fibroblasts cells were examined using the 3-(4, 5-dimethylthiazol-2-yl)-2, 5-diphenyltetrazolium bromide (MTT) colorimetric assay. Primary buccal mucosal fibroblast cells (10,000 cells per well) were seeded into each well of 96-well plate (TPP® Zellkultur and Labortechnologie, Switzerland) followed by incubation at 37 °C for 24 h in 5% CO₂ atmosphere to allow cells to attach or adhere to the bottom of the well plate. The variable concentrations of EGCG and QUR (10, 20, 40, 80, 160 and 320 µM) were prepared in 100 µL of culture medium, added to their respective wells as per the groups, and incubated at 37 °C for 48 h in 5% CO₂ atmosphere. After incubation, the medium was aspirated, and the cells were washed with PBS. Each well in the plate was incubated with 100 µL of MTT solution (5 mg/mL concentration) for 4 h at 37 °C in 5% CO₂ atmosphere. After 4 h, the medium containing MTT solution was aspirated, and DMSO was added to each well to dissolve formazan crystals. The cell viability was analyzed by examining the absorbance at 570 nm and 630 nm using an ELISA plate reader (BioTek Epoch 2 Microplate Spectrophotometer, Agilent, India). All the experiments were performed in triplicates (Kamiloglu et al. 2020). The % cell viability was calculated using the following formula.

$$\% \text{ Cell viability} = (\text{Mean OD value of test sample} / \text{Mean OD value of control sample}) * 100.$$

In vitro efficacy study

The in vitro efficacy of EGCG and QUR was analysed using primary buccal mucosal fibroblast cells. The pure EGCG and QUR were evaluated for mRNA expression of *TGF-β1*, *COL1A2* and *COL3A1* which are overexpressed in the OSF. The fibroblasts were seeded in the 12 well plates and 48 well plates and incubated at 37 °C for 24 h in 5% CO₂ atmosphere. The arecoline hydrobromide solution (25 µg/mL) was supplemented in a culture medium for 48 h to induce fibrosis (Adtani et al. 2017, 2018). After confirmation of OSF induction, cells were treated with pure EGCG (10 µM) and QUR (10 µM) for 24 h and evaluated for mRNA expression of *TGF-β1*, *COL1A2* and *COL3A1* and stained for collagen deposition (Hsieh et al. 2017, 2018).

RNA isolation using RNAiso Plus

The media was removed from the plate, and cells were washed with ice-cold PBS. The RNAiso Plus reagent was used for cells homogenization, and cells were collected into centrifuge tubes by scrapping the plate using cell scraper. Chloroform (molecular biology grade) was added to the above microcentrifuge tube containing cell suspension and properly mixed by vortexing vigorously. The samples were kept for 5 min at room temperature and then centrifuged at 12,000 g and 4°C for 15 min. After centrifugation, the upper layer was separated and collected in another labelled microcentrifuge tube, followed by addition of isopropanol and mixed properly by vortexing vigorously. The vortexed samples were kept at room temperature for 10 min. and centrifuged at 12,000 g for 10 min at 4°C. The obtained RNA pellet was washed with 75% v/v ethanol by centrifugation (Sigma cooling centrifuge) at 4°C, and 7500 g for 5 min and the same procedure was repeated three times to wash the RNA pellet. The pellet was air-dried and dissolved in 20 µL of DEPC-treated water. The concentration of RNA isolated was measured using Biospectrometer (Eppendorf AG, Germany).

Complimentary DNA (cDNA) synthesis

The RNA was converted to cDNA by using Prime Script RT reagent K Perfect (DSS Takara Bio India Pvt. Ltd., New Delhi.) as per the manufacturer's recommended protocol. The master mix was prepared by mixing 5 × PrimeScript buffer, PrimeScript RT enzyme mix I, oligo dT Primer (50 µM), random hexamer (100 µM), RNAase-free dH₂O and total RNA (equivalent to 200 ng of RNA) to get total 20 µL reaction mixture. All the steps followed in dark and under cold conditions. While adding aliquots of the above-prepared mixture into a microcentrifuge tube, followed by

Table 1 Details of nucleotide sequences used in the study

Gene	Primer Sequence (5' → 3')	
<i>TGF-β1</i>	Forward	ACAGCAGGGATAACACAC
	Reverse	GCAATAGTTGGTGTCCAG
<i>COL1A2</i>	Forward	GGAACTCCAGGTCAAACA
	Reverse	ACCCACACTTCCATCACT
<i>COL3A1</i>	Forward	ACTTAGAGGTGGAGCTGGT
	Reverse	TCCAAGACCTCCTCCTTTC
<i>18S</i>	Forward	GTAACCCGTTGAACCCCAT
	Reverse	CCATCCAATCGGTAGTAGCG

TGF-β1 Transforming growth factor beta 1, *COL1A2* Collagen type 1A2, *COL3A1* Collagen type 3A1, *18S* house-keeping gene

the addition of RNA samples. The reaction mixture was incubated for three different duration and temperature conditions, first at 37 °C for 60 min for reverse transcription, second at 85 °C for 5 s for inactivation of reverse transcriptase with heat treatment, and last at 4 °C using Veriti 96 wells Thermal Cycler (Applied Biosystems, Thermo Fisher Scientific).

Real-time polymerase chain reaction (RT-PCR)

For performing the RT-PCR, the mixture was prepared using TB Green *Premix Ex Taq* II (2X), PCR forward primer (10 µM), PCR reverse primer (10 µM), cDNA solution and sterile purified water to get the 20 µL of the reaction mixture. The prepared samples were mixed homogeneously, and RT-PCR was performed in three steps. The first step includes initial denaturation for 30 s at 95 °C, followed by the second step, which includes conditioning of samples for 5 s and 34 s at 95 °C and 60 °C, respectively. The final steps involve dissociation by conditioning samples at three different conditions, 95 °C, 60 °C and 95 °C for 15 s, 60 s, and 15 s, respectively (QuantStudio™, Applied Biosystems, Thermo Fisher Scientific) (Adtani et al. 2018). The details of nucleotide sequences used in the study are given in Table 1.

Masson trichrome staining

After treatment duration, the Masson trichrome staining was performed on the cells using standardized protocol by Lillehei Heart Institute, University of Minnesota, USA (Adtani et al. 2018). Briefly, the media was aspirated from each well, and the cells were washed with DPBS. The cells were fixed in 4% paraformaldehyde at room temperature for 20 min. The fixed cells were washed with distilled water for 1 min. The Weigert's hematoxylin working solution (0.2 mL) was added to each well and kept the plate at room

temperature for 10 min. Further, the solution was aspirated, and the cells were rinsed with distilled water for 10 min. Biebrich scarlet-acid fuchsin solution (0.2 mL) was added to the cells and after 1 min, plate was washed quickly with distilled water. Further, a phosphomolybdic acid–phosphotungstic acid solution was added and incubated the plates at room temperature for 30 min. After aspiration of the solution, aniline blue solution (0.2 mL) was added to the plate and incubated at room temperature for 10 min. The plate was washed quickly with distilled water after aspirating the solution. The cells were treated with 1% v/v acetic acid solution for 4 min. Cells were then washed with 95% v/v alcohol followed by 100% v/v alcohol for 1 min, twice. The stained cells were observed under CKX53 microscope (OLYMPUS Medical Systems India Pvt. Ltd.).

In vivo efficacy studies

Animals

The experimental protocol for in vivo efficacy and safety studies was approved by the Institutional Animal Ethical Committee (IAEC), Kasturba Medical College, MAHE, Manipal (#IAEC/KMC/112/2018). The studies were conducted as per the Committee for the Purpose of Control and Supervision of Experiments on Animals (CPCSEA) guidelines. The studies were performed in two months old male Sprague–Dawley rats weighing 200–250 g. The rats were obtained from the Central Animal Research Facilities, MAHE, Manipal. Three rats were housed per cage made up of propylene with free access to water and food. The temperature and relative humidity conditions were maintained at $25 \pm 1^\circ\text{C}$ and 45–55% relative humidity with a 12 h light/dark cycle.

OSF induction and treatment

Sub-buccal administration of areca nut extract (ANE, 100 μL , 20 mg/mL) was given at the left buccal mucosa of rats on an alternate day for 60 days (Chiang et al. 2020). The control group of rats ($n=6$) did not received ANE, instead water for injection was applied topically thrice a day. The disease control group ($n=6$) received sub-buccal ANE (100 μL , 20 mg/mL) along with the buccal application of water for injection thrice a day. The third set of rats ($n=6$) received sub-buccal ANE (100 μL , 20 mg/mL) along with once-a-week standard treatment betamethasone injection (BTM inj.). The fourth set of rats ($n=6$) received sub-buccal ANE (100 μL , 20 mg/mL) along with thrice a day topical application of EGCG-loaded hydrogel (81.81 mg/kg). Half an hour after the application of formulation or BTM inj, rats were restricted from eating food and drinking water to avoid

swallowing the formulation and to get the local mucoadhesive action of formulations on the buccal mucosa. The treatment procedure was followed for 90 days to assess the efficacy of the EGCG-loaded hydrogel (El-feky and Zayed 2019), and mucosal samples were collected from different groups of rats at the end of 90 days of treatment. During the treatment period, the rats were analysed for body weight (using a digital weighing balance) and mouth opening (using a digital Vernier caliper) once a week. After 90 days of treatment, the rats were killed, and buccal mucosa was harvested, which was used for histopathological studies by hematoxylin and eosin (H and E) and Masson trichrome method (Shekatkar et al. 2022). The concentration of collagen type-1, and TGF- β 1, in the collected tissue samples, was estimated by ELISA kit (Maxome Labsciences, India, and Elabscience, India). The oxidative stress markers such as nitric oxide (NO), superoxide dismutase (SOD), catalase (CAT), thiobarbituric acid reactive substance (TBARS), 2,2-diphenyl-1-picryl-hydrazyl-hydrate (DPPH), glutathione activity and ferric reducing antioxidant power (FRAP) were analysed in tissue samples by standard methods.

Statistical analysis

All experimental studies were performed in triplicates, and the results were represented as mean and standard deviation. GraphPad Prism 8.0.2 was used for performing the statistical analysis. The results were analyzed according to the one-way ANOVA and considered significant if $p < 0.05$.

Results

Protein preparation and binding site identification

The SiteMap identified the ligand-binding pockets on the selected target protein, and based on the pocket environment analysis, the site-score and D-score were calculated for each pocket. The site-score is a measure of a particular site being the ligand-binding site, and the D-score indicates the druggability of a particular pocket (Halgren 2007, 2009). The site-score value of more than 1.0, implies a high probability that it could be a ligand-binding site. If the score is between 0.7 and 1.0, it is a partial ligand-binding site; if the score is less than 0.7, it is a non-ligand-binding site. A D-score of more than 1.0 indicates that the pocket is a druggable binding site; if it is between 0.7 and 1.0, it is a partially druggable site, and if the score is less than 0.7, it is a non-druggable site. The LOX protein was found to have three binding pockets with a site-score of

Table 2 Intermolecular interaction pattern of selected polyphenols on LOX protein

Proteins	LOX site-1			LOX site-2			LOX site-3		
	HB	HP	π - π stacking	HB	HP	π - π stacking	HB	HP	π - π stacking
EGCG	GLY330	ILE334	ARG478	ILE334	TYR333	LYS373	GLU346	–	HIP747
	GLY331	MET474		GLU336	MET429		ILE388		
	ALA332	PHE484		ARG423			SER411		
	GLY483	TYR725		CYS424			GLU555		
	SER512			THR426			ILE748		
	SER723			GLY483			SER751		
	SER726								
QUR	GLY330	ARG329	–	GLU336	TYR333	–	ARG329	ILE385	–
	GLY331	VAL471		CYS424	ILE334		ARG338	VAL551	
	ARG478	MET474		LEU431	LYS373		GLU340	ILE748	
	SER512	TYR725		GLN479			ILE748		
	ASP724								
CUR	GLY330	TYR72	–	ILE334	TYR333	–	ARG338	ILE385	–
	ARG478	MET474		ARG478			ARG339		
	SER512	VAL713		GLN479			GLU340		
	PRO716	PHE718					ILE748		
RSV	GLY330	ARG329	–	GLN479	ILE334	–	GLU340	ILE385	–
	TYR333	ARG478			ALA428		GLU346	PRO387	
	GLY335				MET429		ALA554		
	GLU336						GLU555		
	ASP724								
MAT	ARG478	LEU328	–	THR426	PRO427	–	GLU555	TRP347	–
	SER723	GLY331		ARG478	ALA428		SER751	PRO387	
		ALA332		GLN479	MET429			ALA554	
		MET474						ILE748	
		PHE484							
LYP	ARG329	GLY331	–	ARG478	PRO427	–	ARG329	TRP347	–
	SER723	MET474		GLN479	MET429		GLU340	PRO387	
		TYR725			ILE334		ASN727	ALA554	
							ILE748		

EGCG epigallocatechin 3-gallate, QUR quercetin, CUR curcumin, RSV resveratrol, MAT matrine, LYP lycopene, LOX lysyl oxidase, HB H-bonds, HP hydrophobic interaction, LYS lysine, ASP aspartic acid, ASN asparagine, ILE isoleucine, VAL valine, SER serine, HIS histidine, GLY glycine, TYR tyrosine, ALA alanine, LEU leucine, CYS cysteine, MET methionine, TRP tryptophan, THR threonine, ASN asparagine, ARG arginine, GLU glutamic acid

0.981, 0.975 and 1.040, while the D score for the same was 1.004, 0.945 and 1.060, respectively.

Molecular docking studies

The ligand-binding site was unknown for LOX (PDB ID: 5ZE3) protein (Zhang et al. 2018). The SiteMap analysis identified three druggable ligand sites, site-1, site-2 and site-3. The polyphenols were docked on all three sites identified. The ligands were analyzed for intermolecular interaction with the protein individually at all the binding sites of LOX and TGF- β 1. Among all polyphenols, the EGCG exhibited the highest number of combinations of polar and non-polar type of intermolecular interactions at all the binding sites of LOX and TGF- β 1. The interaction pattern of all the polyphenols with LOX and TGF- β 1

proteins is listed in Tables 2 and 3, respectively. Based on the interaction pattern observed across all the binding sites during molecular docking, the order of binding affinity for polyphenols towards the LOX and TGF- β 1 protein is EGCG > QUR > RSV > CUR > MAT > LYP. EGCG and QUR ranked first and second for all the protein targets exhibiting higher binding interactions, whereas MAT and LYP ranked last. To further confirm the binding stability with the protein at a particular binding site, the four top-ranked polyphenols, EGCG, QUR, RSV and CUR, were subjected to the MD simulation for 100 ns.

MD simulations

In the case of LOX, there were three binding sites identified in LOX, and all the polyphenols, namely, EGCG, QUR, RSV and CUR complexes with LOX at site-1, site-2, and

site-3, were subjected to 100 ns MD simulation. The initial 20 ns were omitted by considering equilibration simulation for all the MD simulation runs. Except for EGCG and CUR, the RMSD fluctuations observed for the polyphenols were higher than 2 Å at the binding site-1. At binding site-2, the RMSD fluctuations were above 2 Å for all the polyphenols. EGCG exhibited higher RMSD fluctuations at the last phase of 70–100 ns simulation, whereas QUR exhibited higher fluctuations between 20 and 35 ns and the last phase of 80–100 ns simulation. At binding site-3, all the polyphenols exhibited a stable binding where the RMSD fluctuations remained at 2 Å. Figure 1 depicts the RMSD plot for the protein backbone and all the polyphenols and Fig. 2 illustrates the protein–ligand contacts between LOX protein and different ligands. The intermolecular interactions observed between the ligands and the different binding sites of LOX protein are listed in Table 4.

EGCG, QUR, RSV, CUR complexes with TGF-β1 protein binding site were subjected to 100 ns MD simulation. The initial 20 ns simulation was omitted by considering the equilibration simulation for all the MD simulation runs. At TGF-β1 binding site, all the polyphenols under study exhibited a stable binding whereas the RMSD fluctuations remained within 2 Å. Figure 3 depicts the RMSD plot for the protein backbone and all the polyphenols, and Fig. 4 depicts the protein–ligand contacts between TGF-β1 protein and different ligands. Overall, considering TGF-β1 binding site, EGCG and RSV exhibited a stable binding compared

to the polyphenols under study. The interactions observed in the trajectory frames generated during MD simulation were similar to those observed during molecular docking. The simulation interaction diagram analysis for TGF-β1 protein is shown in Table 5.

The polyphenols were scored based on binding interactions and binding stability with the target proteins based on the MD simulation studies. From the results, it was observed that all the polyphenols showed stable interactions over TGF-β1. In the case of LOX protein, EGCG interacted to a greater extent with all sites, while QUR, CUR and RSV exhibited stable interactions or binding with only site-3 as compared to site-1 and site-2. Based on these interactions, the overall scoring of the polyphenols was carried out by considering the binding of a polyphenol at the individual binding sites of each target protein. EGCG showed a higher number of interactions (4 times, 4A) as compared to the rest of the polyphenols, and therefore it was given the first rank, QUR, CUR, and RSV showed an equal number of excellent interactions (2 times, 2A), but QUR showed good interactions (2 times, 2B) as compared to CUR and RSV, thus QUR was ranked second and at last RSV and CUR showed equal better and bad interactions (1 times each, 1C and 1D) therefore they were ranked third and fourth in the list. The scoring of the selected polyphenols towards the binding site of each of the proteins is given in Table 6. The following order for the stability of polyphenols (ligands) on the selected

Table 3 Intermolecular interaction pattern of selected polyphenols on TGF-β1 protein

Ligands	HB	HP	π - π stacking
EGCG	LYS232 SER280 ASP281 HIS283 ASP290 LYS335 ASN338 ASP351	ILE211 VAL219 LEU260 LEU340	–
QUR	GLU245 TYR249 ASP281 HIS283 ASP290 ASP351	ILE211 ALA230 LEU260 LEU340	–
CUR	SER80 GLU245 HIS283 ASP290	ILE211 VAL219 LEU260 TYR282	–
RSV	GLU245 TYR249 SER280 HIS283 ASP290 ASP351	ILE211 VAL219 LEU260 LEU340	–
MAT	SER287 ASP290 LYS337	ILE211 VAL219 ALA230 GLY286 LEU340	–
LYP	TYR282 GLU284 ASP290 ARG294 LYS337	ILE211 ALA230 LEU278 PHE289	–

EGCG epigallocatechin 3-gallate, QUR quercetin, CUR curcumin, RSV resveratrol, MAT matrine, LYP lycopene, LOX lysyl oxidase, HB H-bonds, HP hydrophobic interaction, LYS lysine, ASP aspartic acid, ASN asparagine, ILE isoleucine, VAL valine, SER serine, HIS histidine, GLY glycine, TYR tyrosine, ALA alanine, LEU leucine, CYS cysteine, MET methionine, TRP tryptophan, THR threonine, ASN asparagine, ARG arginine, GLU glutamic acid

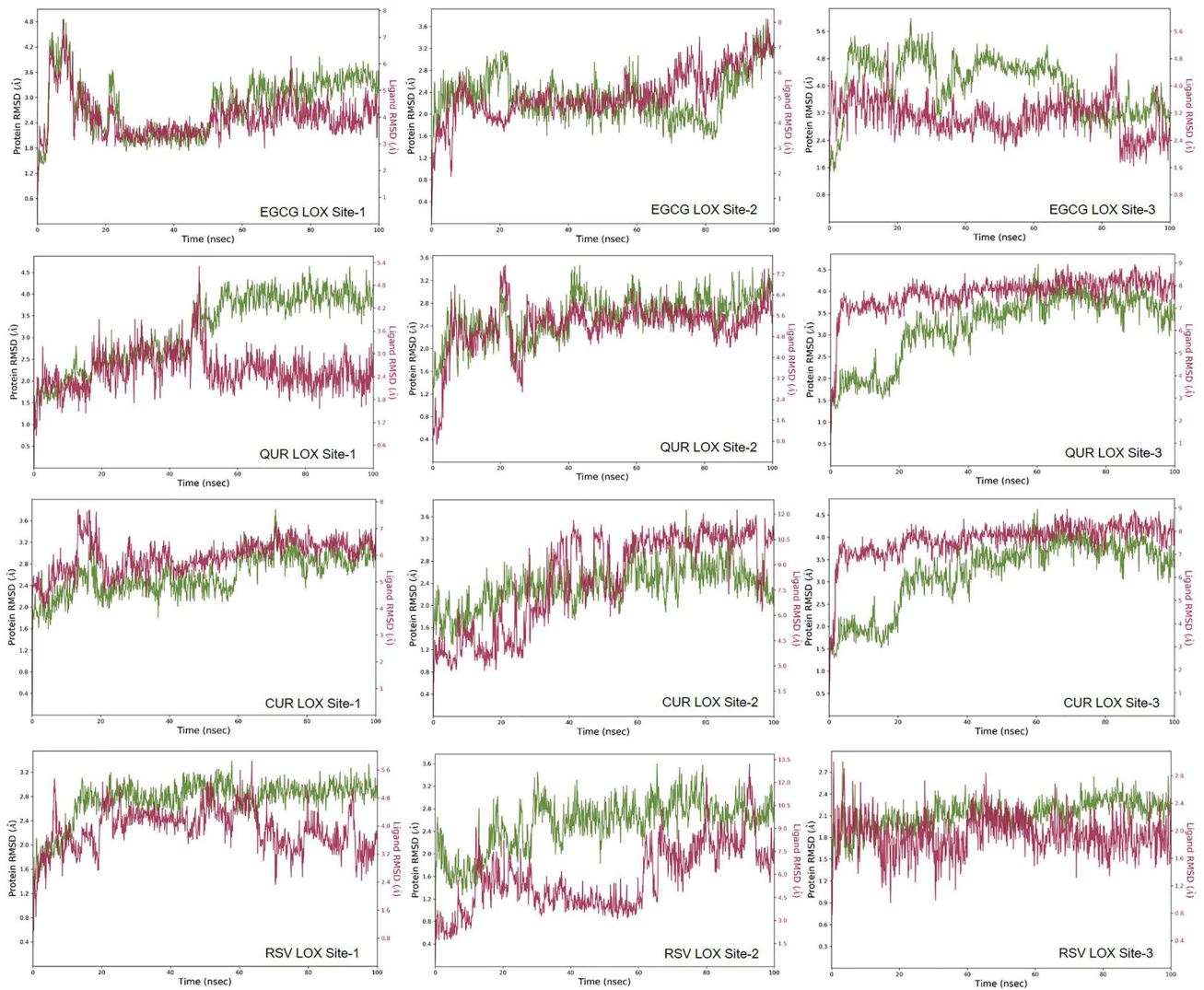


Fig. 1 RMSD observed for the ligand (red) and the LOX protein backbone (green) during the 100 ns MD simulation. *EGCG—epigallocatechin 3-gallate, QUR—quercetin, CUR—curcumin, RSV—resveratrol, MAT—matrine, LYP—lycopene, LOX—lysyl oxidase

proteins was observed: EGCG > QUR > RSV > CUR. The order of interactions indicates that EGCG demonstrated higher structural stability of the complex and the binding mode stability with all the selected proteins.

In vitro cell line studies

In vitro cytotoxicity studies

The primary buccal mucosal fibroblasts cells were successfully extracted from the buccal tissue and used for analysis of EGCG and QUR efficacy on the cells. The effect of EGCG and QUR on cell viability of primary buccal mucosal

fibroblast cells was evaluated using MTT colorimetric assay which suggested that EGCG and QUR at 10 μM concentration did not induce cytotoxicity in the cells whereas at 320 μM decreased cell viability (57.25 and 1.55% cell viability, respectively for EGCG and QUR). The IC_{50} values for EGCG and QUR was calculated to 342.3 and 109.1 μM , respectively. Overall, EGCG was found to be safer as compared to QUR. Based on this data, the safer concentration 10 μM was considered for further studies, including in vitro efficacy and Masson's trichrome staining studies. There was no statistically significant difference observed when different concentration groups were compared. The results of in vitro cytotoxicity at different concentrations of EGCG and QUR is shown in Fig. 5.

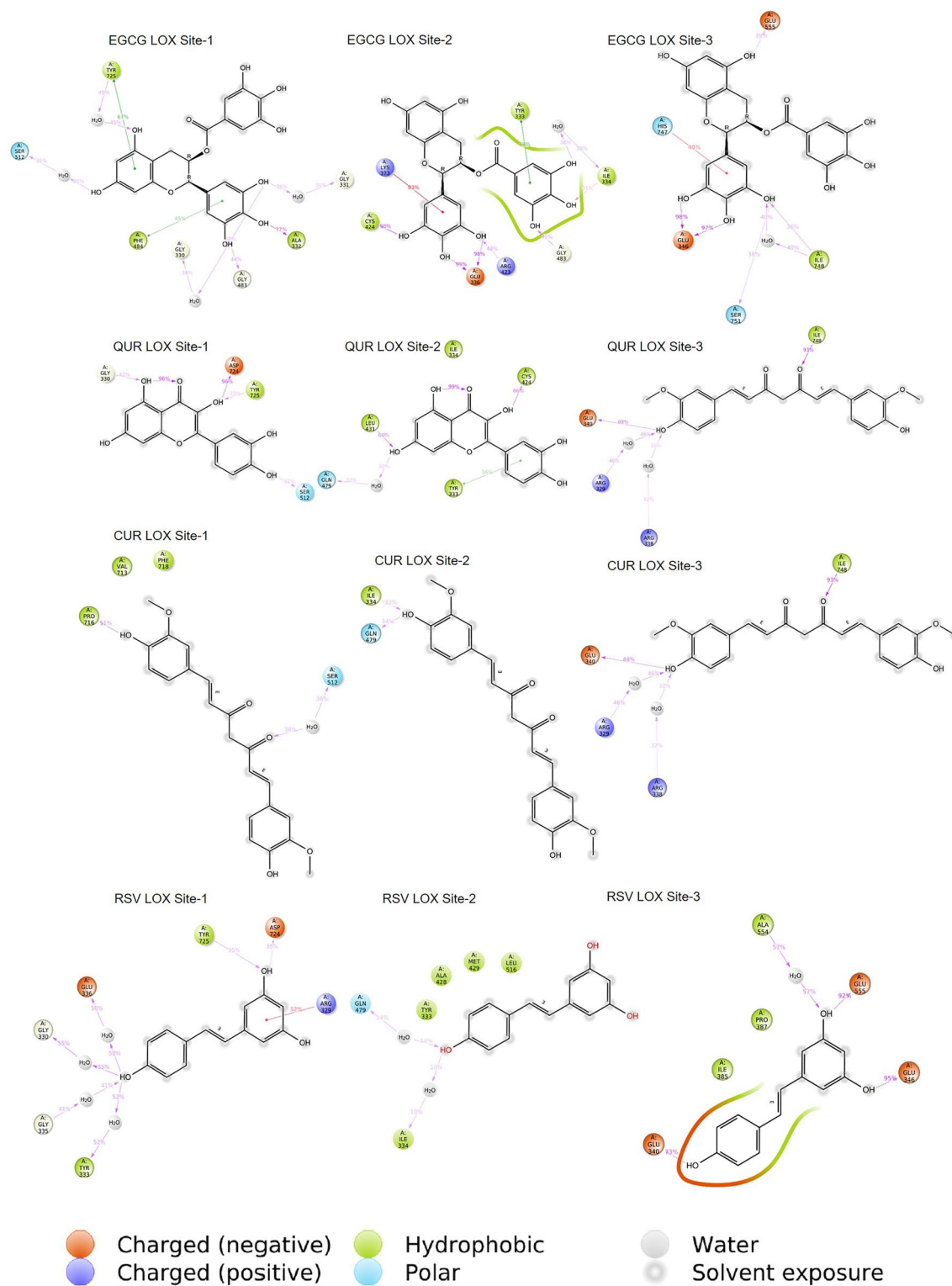


Fig. 2 Protein–ligand contacts between LOX protein and ligands. EGCG—epigallocatechin 3-gallate, QUR—quercetin, CUR—curcumin, RSV—resveratrol, MAT—matrine, LYP—lycopene, LOX—lysyl oxidase

Table 4 Simulation interaction diagram analysis for LOX protein

Ligand protein complex	P–L RMSD	P–L Contacts (%)			Ranking
		HB	HP	WB	
EGCG LOX site-1	Stable	80.9 (ALA332) 50 (ARG478) 40 (GLY483)	30 (ILE334) 68.9 (PHE484) 80.8 (TYR725)	40 (GLY330) 30 (GLY331) 40 (SER512) 30 (SER723) 30 (SER726)	A
EGCG LOX site-2	Stable	94.6 (ILE334) 198.2 (GLU336) 40 (ARG423) 90 (CYS424) 68.9 (GLY483)	125.3 (TYR333) 84.2 (LYS373) 30 (MET429)	40 (ILE334) 50 (THR426)	A
EGCG LOX site-3	Stable	196.2 (GLU346) 40 (GLU555) 40 (SER751) 40 (ILE748)	50 (HIS747)	40 (ILE388) 40 (SER411)	A
QUR LOX site-1	Stable	45 (GLY330) 96 (ASP724)	30 (TYR725)	55 (GLY330)	B
QUR LOX site-2	Stable	68.8 (CYS424) 68 (LEU431)	68 (TYR333) 30 (ILE334)	30 (GLN479)	B
QUR LOX site-3	Stable	68.1 (GLU340) 94.7 (ILE748)	67.5 (ILE385)	65.4 (ARG329) 45 (ARG338)	A
CUR LOX site-1	Stable	55 (PRO716)	66.6 (PHE718) 40 (VAL713)	40 (SER512)	C
CUR LOX site-2	Unstable	30 (ILE334) 35 (GLN479)	50 (TYR333)	-	D
CUR LOX site-3	Stable	68.1 (GLU340) 94.7 (ILE748)	67.5 (ILE385)	65.4 (ARG329) 35 (ARG338)	A
RSV LOX site-1	Stable	35 (ASP 724) 30 (TYR725)	50 (ARG329)	50 (GLY330) 50 (TYR333) 40 (GLU336)	C
RSV LOX site-2	Unstable	-	30 (ILE334)	-	D
RSV LOX site-3	Stable	73.9 (GLU340) 95.9 (GLU346) 92.3 (GLU555)	40 (ILE385) 50 (PRO387)	50 (ALA554)	A

EGCG epigallocatechin 3-gallate, QUR quercetin, CUR curcumin, RSV resveratrol, Mat matrine, LYP Lycopene, LOX lysyl oxidase, HB H-bonds, HP hydrophobic interaction, P–L protein–ligand, RMSD root mean square deviation, LYS lysine, ASP aspartic acid, ASN asparagine, ILE isoleucine, VAL valine, SER serine, HIS histidine, GLY glycine, TYR tyrosine, ALA alanine, LEU leucine, CYS cysteine, MET methionine, TRP tryptophan, THR threonine, ASN asparagine, ARG arginine, GLU glutamic acid

Masson's trichrome staining

Masson's trichrome staining was performed to analyze the qualitative effect of EGCG and QUR treatment on the collagen deposition using primary buccal mucosal fibroblast cells. The qualitative effect of post-treatment with EGCG and QUR (10 μ M) was evaluated on the pre-treated fibroblast cells with arecoline hydrobromide (25 μ g/mL). The control group (G1) stained faintly for collagen deposition, while arecoline-treated group (G2) showed stronger staining due to higher collagen deposition. In comparison to the arecoline-treated group (G2), EGCG (G3)- and QUR (G4)-treated groups showed better improvement in collagen reduction by showing faint staining for collagen. The Masson's trichrome staining for comparing collagen

production qualitatively between different groups is shown in Fig. 6.

In vitro efficacy studies

The effect of EGCG and QUR on the arecoline-induced OSF in vitro model was evaluated by the mRNA expression of *TGF- β 1*, *COL1A2* and *COL3A1* in primary buccal mucosal fibroblast. Based on the literature, arecoline hydrobromide at 25 μ g/mL was used (Adtani et al. 2018). After confirmation of fibrosis induction by 48 h, the cells were treated with 10 μ M of EGCG and QUR for 24 h and after required duration, the mRNA expression of *TGF- β 1*, *COL1A2* and *COL3A1* was evaluated. The mRNA expression levels of *TGF- β 1*, *COL1A2* and *COL3A1* between different groups is shown in Fig. 7. The

Fig. 3 RMSD deviations observed for the ligand (red) and the TGF- β 1 proteins backbone (green) during the 100 ns MD simulation; EGCG—epigallocatechin 3-gallate, QUR—quercetin, CUR—curcumin, RSV—resveratrol, TGF- β 1—transforming growth factor- β 1

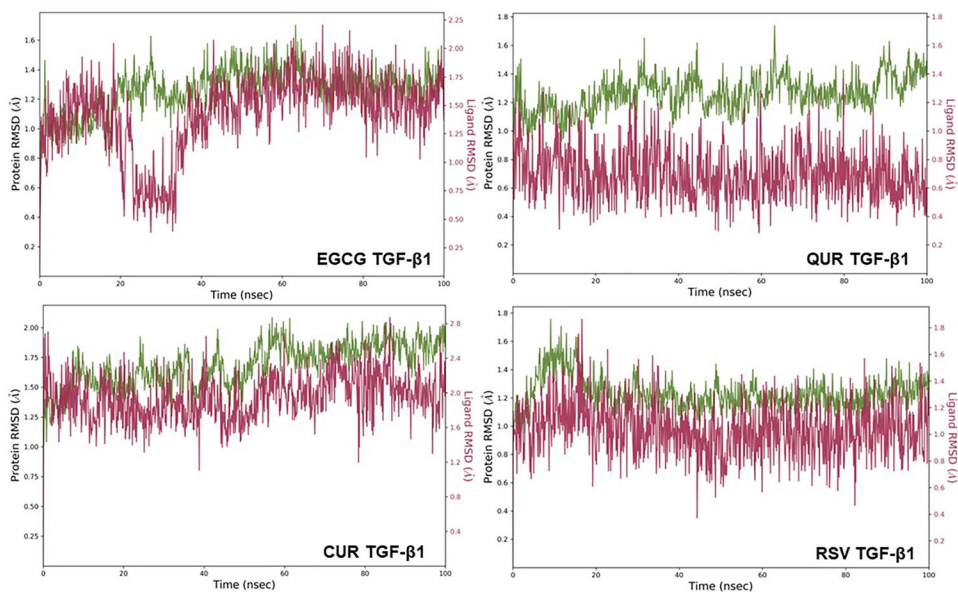


Fig. 4 Protein–ligand contacts between TGF- β 1 protein and ligands; EGCG—Epigallocatechin 3-gallate, QUR—quercetin, CUR—curcumin, RSV—resveratrol, TGF- β 1—transforming growth factor- β 1

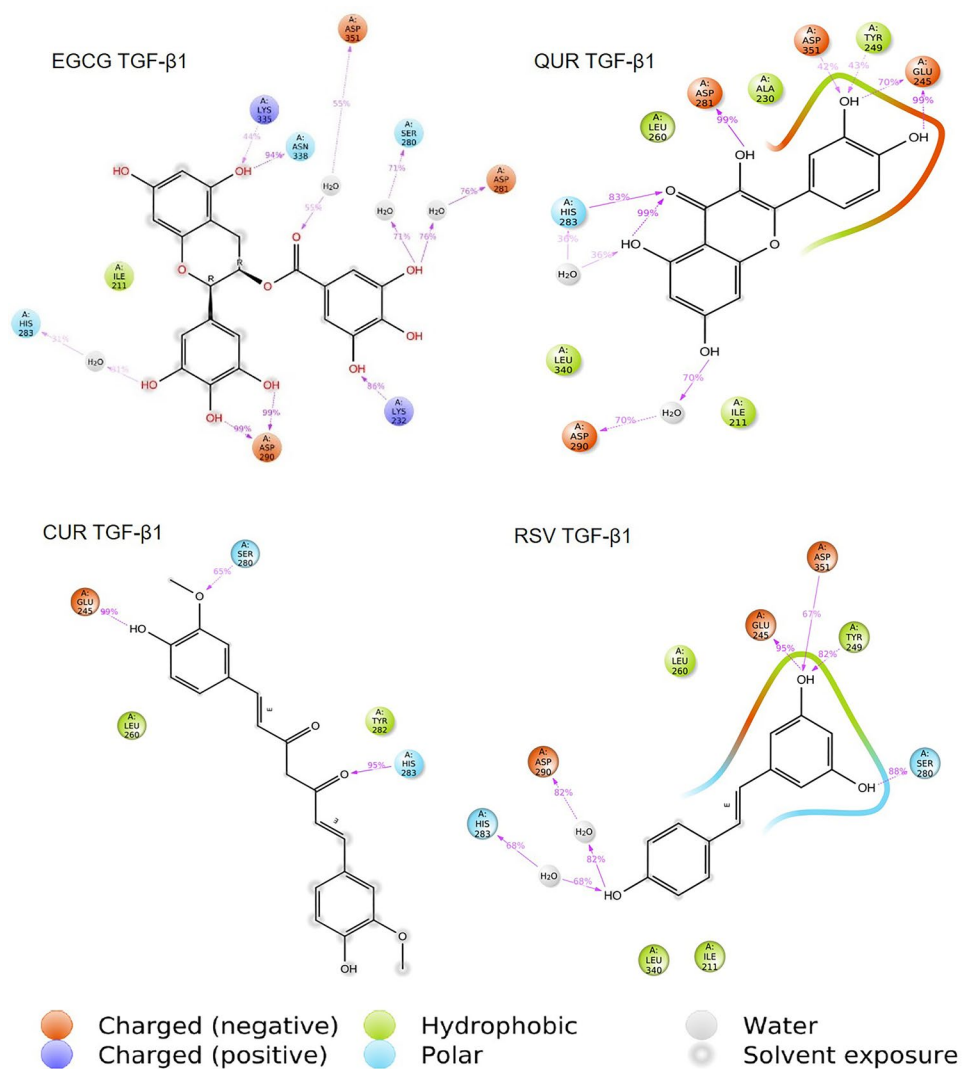


Table 5 Simulation interaction diagram analysis for TGF- β 1 protein

Ligand protein complex	P-L RMSD	P-L Contacts (%)			Ranking
		HB	HP	WB	
EGCG TGF- β 1	Stable	86.3 (LYS232) 198.3 (ASP290) 40 (LYS335) 94.7 (ASN338)	50 (ILE211) 30 (VAL219)	87.5 (SER280) 91.3 (ASP281) 50 (HIS283) 40 (ASP351)	A
QUR TGF- β 1	Stable	170.7 (GLU245) 40 (TYR249) 99.8 (ASP281) 101.8 (HIS283) 71.2 (ASP351)	40 (ILE211) 60.6 (ALA230) 67.2 (LEU260) 50 (LEU340)	90.7 (ASP290)	A
CUR TGF- β 1	Stable	99.3 (GLU245) 65.3 (SER280) 100.4 (HIS283)	30 (ILE211) 30 (VAL219) 55 (LEU260) 66.1 (TYR282)	40 (ASP290)	A
RSV TGF- β 1	Stable	95.1 (GLU245) 82.2 (TYR249) 88.4 (SER280) 2.8 (ASP351)	30 (ILE211) 55 (LEU260) 40 (LEU340)	69.3 (HIS283) 82.9 (ASP290)	A

EGCG epigallocatechin 3-gallate, QUR quercetin, CUR curcumin, RSV resveratrol, MAT matrine, LYP lycopene, TIMP tissue inhibitor of the matrix metalloproteinase, HB H-bonds, HP hydrophobic interaction, P-L protein-Ligand, RMSD root mean square deviation. LYS lysine, ASP aspartic acid, ASN asparagine, ILE isoleucine, VAL valine, SER serine, HIS histidine, GLY glycine, TYR tyrosine, ALA alanine, LEU leucine, CYS cysteine, MET methionine, TRP tryptophan, THR threonine, ASN asparagine, ARG arginine, GLU glutamic acid

mRNA expression of *TGF- β 1*, *COL1A2* and *COL3A1* significantly ($p < 0.05$) increased in the arecoline-treated group (G2) compared to the control (G1), confirming the induction of fibrosis. Treatment with 10 μ M of EGCG (G3) significantly ($p < 0.05$) reduced mRNA expression of *TGF- β 1*, *COL1A2* and *COL3A1* compared to disease control (arecoline treated group, G2). There was significant ($p < 0.05$) decrease in mRNA expression of *COL1A2* and *COL3A1* in QUR treated group (G4) compared to the disease control group (arecoline treated, G2). EGCG showed better improvement in disease conditions by significantly reducing the mRNA expression of *TGF- β 1*, *COL1A2* and *COL3A1*. The earlier research work performed by Hsieh and their group suggested that EGCG exhibited a promising role in inhibiting *TGF- β 1*-induced collagen synthesis by suppressing early growth response-1 (EGR-1) when evaluated on human buccal mucosal fibroblasts.

In vivo efficacy studies

The efficacy of EGCG was studied in ANE induced rat OSF model. The mortality was not observed in rats during the OSF induction as well as throughout the treatment period. The changes observed in rat weight (g) and mouth opening (cm), which were evaluated every week during treatment, are shown graphically in Fig. 8. EGCG hydrogel treatment did not produce a major difference in the weight

of rats, and mouth opening compared to the control rats. EGCG hydrogel treatment showed better improvement in the mouth opening compared to BTM inj. It was also noticed that there were local infections in the oral cavities of BTM inj. treated rats. Induction of OSF in the rats required two months which was confirmed by a decrease in mouth opening and increase in TGF- β 1 and collagen type-1 in the disease control rats. Figure 9 represents the TGF- β 1 and collagen-1 concentrations in oral submucosal tissue upon treatment with BTM inj. and EGCG hydrogel. There was significant increase in TGF- β 1, and collagen type-1 in the disease control group compared to the normal control group. The TGF- β 1 and collagen type-1 in OSF-induced rats were significantly lower in EGCG hydrogel and BTM inj., compared to the OSF induced rats. Both EGCG hydrogel and BTM inj. showed an almost equal reduction in overexpression of TGF- β 1 and collagen type-1.

Figure 10 represents the antioxidant parameters in the oral submucosal tissues of rats. NO, TBARS, FRAP and glutathione were found to be higher in the disease control rats compared to the normal rats, while EGCG hydrogel and BTM inj. prevented this and did not produce any significant changes compared to normal rats. The SOD, catalase, and %DPPH scavenging was found significantly decreased in the disease control rats compared with the normal control rats. There was a significant improvement in SOD and %DPPH upon treatment with EGCG hydrogel, while there

Table 6 Scoring of different polyphenols (ligands) based on simulation interaction diagram

Proteins	Ligands (Scoring)			
	EGCG	QUR	CUR	RSV
LOX site-1	A	B	C	C
LOX site-2	A	B	D	D
LOX site-3	A	A	A	A
TGF- β 1	A	A	A	A
Total scoring	4A	2A and 2B	2A, 1C and 1D	2A, 1C and 1D

A = excellent, B = good, C = better and D = bad or no interactions

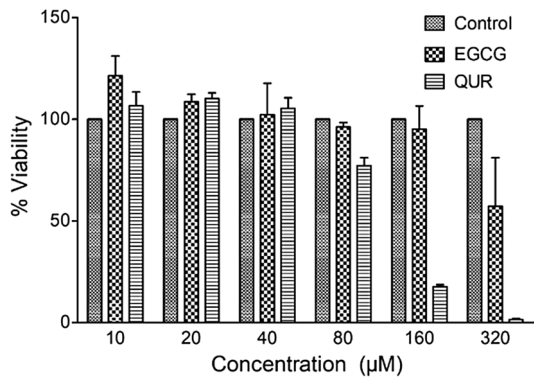
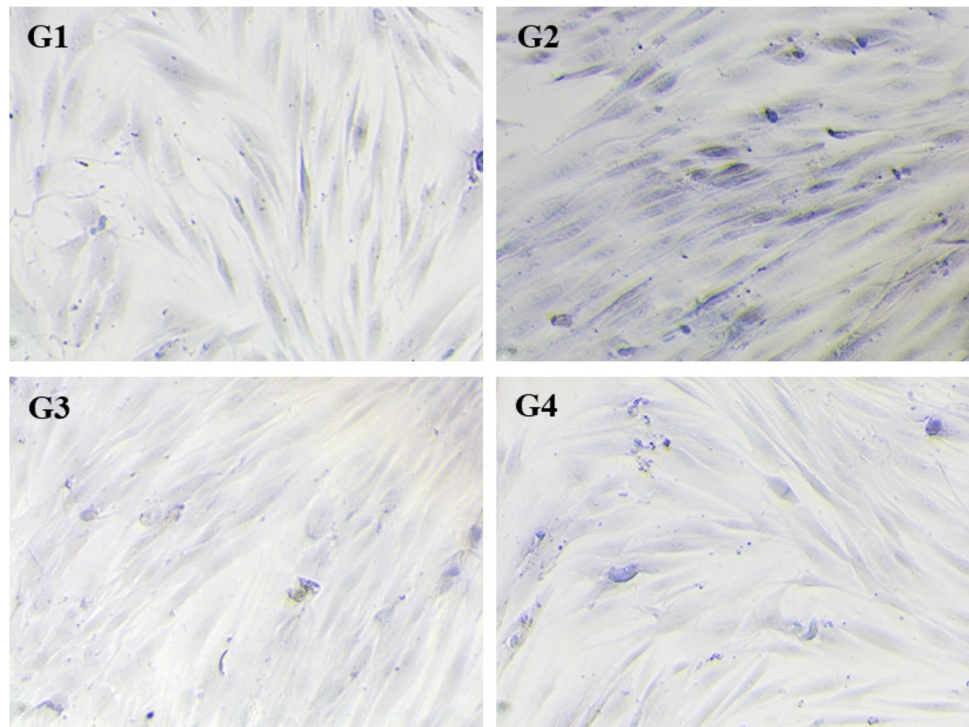


Fig. 5 Cytotoxicity of EGCG and QUR on primary buccal mucosal fibroblasts. Values are Mean \pm SD; Control: cells without treatment; EGCG: epigallocatechin 3-gallate treated; QUR: quercetin treated

Fig. 6 Masson's trichrome staining of primary buccal mucosal fibroblast. Comparison of collagen production qualitatively between control (G1), disease control (arecoline treated, G2) and treatment with EGCG (G3) and QUR (G4); EGCG: epigallocatechin 3-gallate; QUR: Quercetin. All the images were captured at a magnification of 100 μ (10X)



was no much difference observed in BTM inj. compared to disease control rats. There was significant protection in catalase upon BTM inj.; however, the protection was not significant by treatment with EGCG hydrogel compared to disease control group.

Figure 11 represents the histopathological evaluation by using hematoxylin and eosin (H and E) staining and Masson trichrome staining. The histology of control group showed 10–16 layers of thickness ($183.83 \pm 29.29 \mu\text{m}$) stratified squamous keratinized epithelium with rete ridges. The connective tissue beneath the epithelium showed few blood vessels and muscle fibers. Whereas the disease control group showed 3–6-layered thick ($44.66 \pm 36.48 \mu\text{m}$) ulcerative epithelium with the presence of scab which showed fibrin and cell debris, the large necrosed area in the dermis, granulomatous inflammation with giant cells, an abundance of chronic inflammatory cells like lymphocytes, congested blood vessels. The histopathology from rats treated with BTM inj. showed atrophic epithelium with 3–6 layers thickness ($67.51 \pm 11.28 \mu\text{m}$), the connective tissue beneath the epithelium showed dense infiltration of lymphocytes, muscle fibers, and mild fibrosis areas were seen. In the histology obtained from rats treated with EGCG has stratified squamous epithelium consisting of 3–6 cell layers thickness ($76.02 \pm 34.76 \mu\text{m}$) with an atrophic region. The rete ridges in the epithelium was absent and, lymphocytic infiltrates, congested blood vessels, and many macrophages were seen in the dermis. Fibrosed areas were seen in the dermis. The histology of

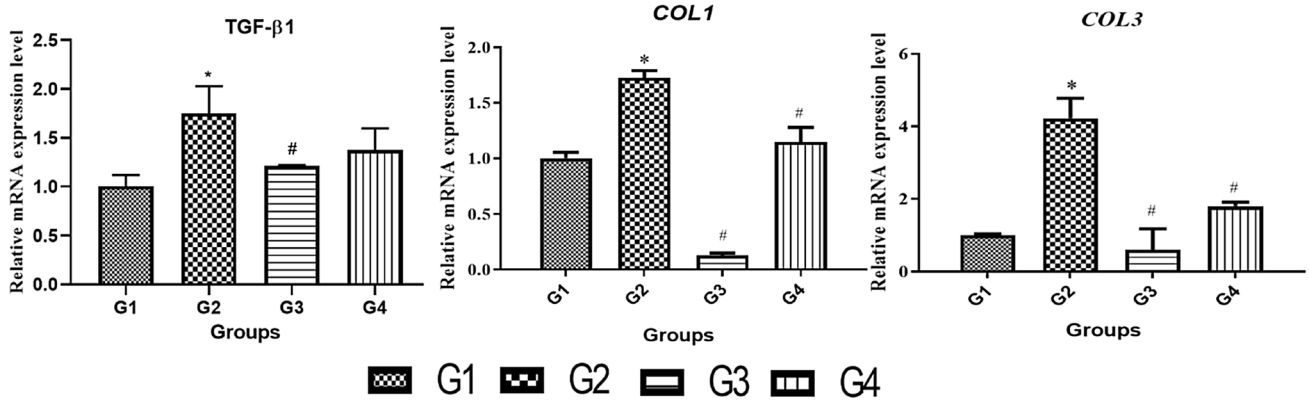


Fig. 7 mRNA expression of *TGF-β1*, *COL1A2* and *COL3A1* in primary buccal mucosal fibroblasts. Comparison between control (G1), disease control (arecoline treated, G2), treatment groups (EGCG

treated group (G3) and QUR treated group (G4); * $p < 0.05$ compared to G1, # $p < 0.05$ compared to G2

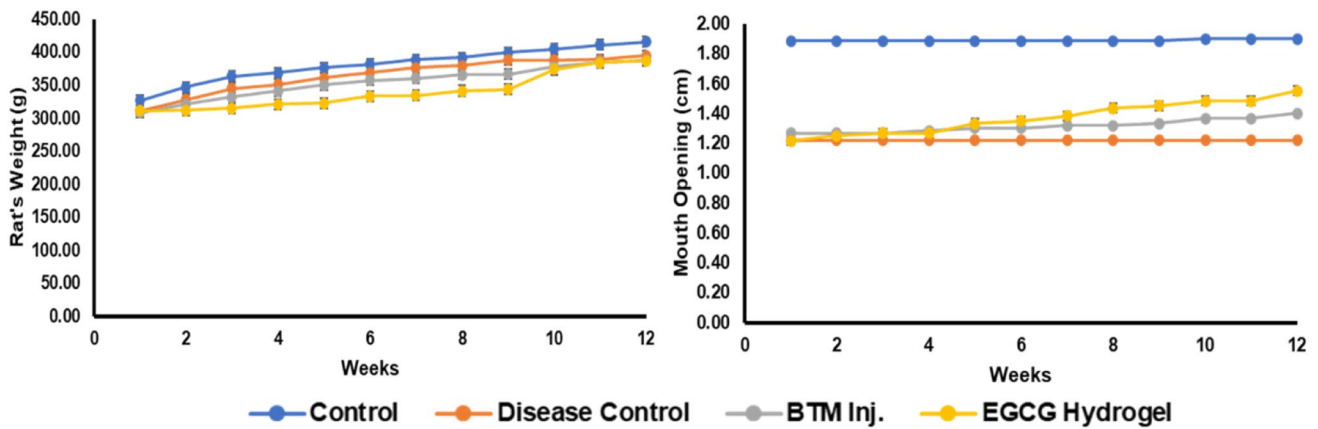
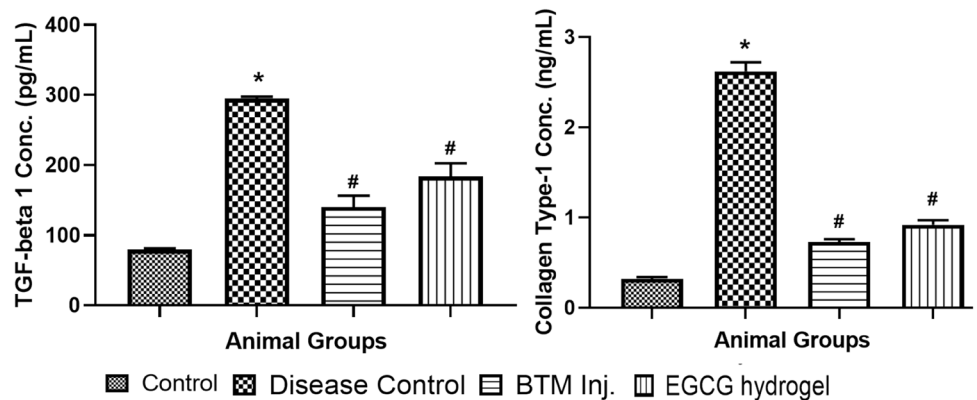


Fig. 8 Evaluation of rat's weight (g) and mouth opening (cm) at different time intervals (weekly), BTM Inj.—betamethasone injection

Fig. 9 TGF-β1 and collagen-1 concentration in various animal groups. * $p < 0.0001$ compared to control group. # $p < 0.0001$ compared to disease control group



rats in the disease control group showed the tight arrangement of collagen fibres in buccal mucosal region while normal control group showed loosely arranged collagen

fibres. The BTM inj. and EGCG hydrogel treated rats showed a tight arrangement of collagen fibres in buccal mucosa.

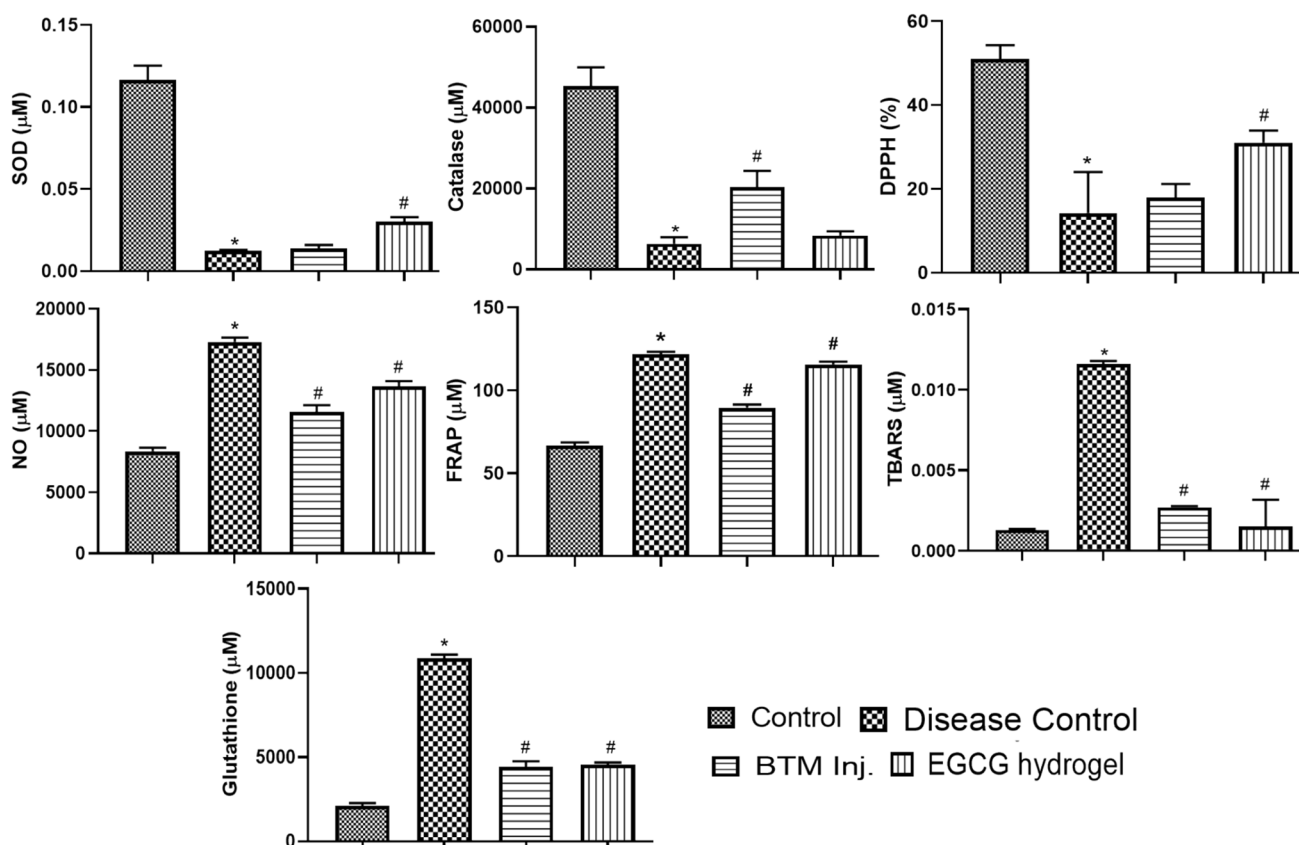


Fig. 10 Antioxidant assays for different animal groups. * $p < 0.0001$ compared to control group, # $p < 0.0001$ compared to disease control group

Discussion

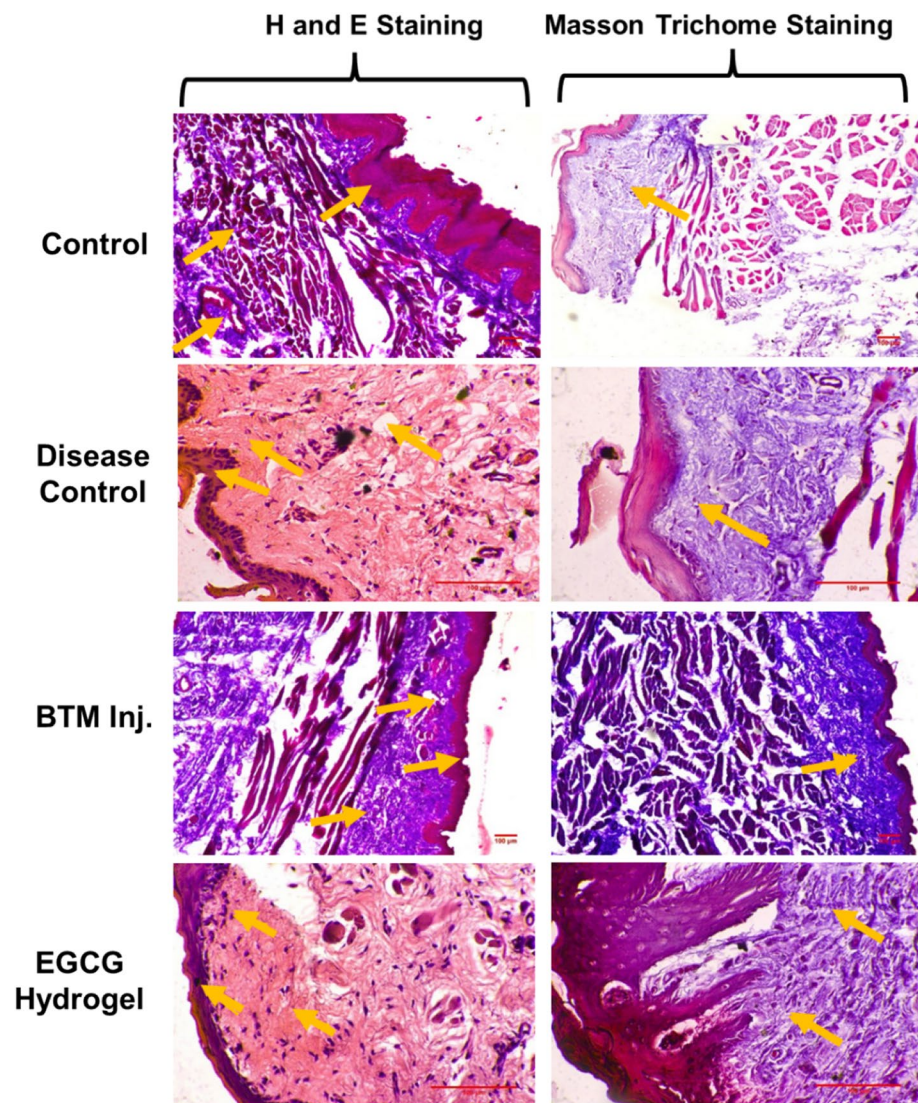
The combination of *in silico*, *in vitro* and *in vivo* studies were performed for the selection of potential molecule and examination of its efficacy using primary buccal mucosal fibroblasts cells and ANE induces OSF rat model, respectively. To explore the nature of polypharmacology by polyphenols, *in silico* tools were used, and the study revealed that these polyphenols could be able to tightly bind to multiple drug targets such as TGF- β 1 and LOX. The docking scores and MD simulation studies revealed, EGCG, QUR, CUR, and RSV as the top polyphenols. Further, based on the amino acid interactions, binding nature and the visual observation of ligand–protein interactions, EGCG and QUR were shortlisted for *in vitro* studies.

The main objective of the testing the cytotoxicity of the EGCG and QUR was to know the safer concentration of the compounds used. In the preliminary *in vitro* studies, EGCG showed cytotoxicity at lower concentration and QUR required higher concentration to induce the cytotoxicity on cultured human primary buccal fibroblasts. The primary buccal mucosal fibroblasts were used to see the arecoline induced cytosolic changes such as collagen deposition as detected by Masson's trichrome stain. It is the principle

marker for antifibrotic activity (Adtani et al. 2019). The photomicrograms taken clearly differentiated the normal and arecoline induced fibroblastic changes. Both EGCG and QUR have prevented these changes which is evident from the microscopic analysis. Further, EGCG significantly lowered TGF- β 1, but, QUR could not lower it significantly. Hence, EGCG was selected for the *in vivo* studies. However, both EGCG and QUR had significantly lowered mRNA expression for *COL1A2* and *COL3A1*.

The results were in according to the reported literature. Hsieh and group suggested that EGCG exhibited promising role in inhibiting TGF- β 1 induced collagen synthesis by suppressing early growth response-1 (EGR-1) when evaluated on human buccal mucosal fibroblasts. They also investigated the pathways of TGF- β -induced EGR-1 expression in normal human fibroblasts and the effect of EGR-1 inhibition on the expression of *TGF- β 1*. The results showed that at a concentration of 10 μM , EGCG was capable of completely attenuating the production of collagen stimulated by TGF- β 1-induced EGR-1 activation in fibroblasts (Hsieh et al. 2017). They concluded that Egr-1 may be one of the key mediators of TGF- β 1 stimulated fibrosis in OSF which could be a novel target for the treatment of OSF. Hence, based on this evidence, EGCG could be used as a possible

Fig. 11 Histopathology of buccal mucosa in ANE induced OSF rats. H&E and Masson trichrome staining; The OSF was induced in rats by sub-buccal administration of ANE (100 μ L, 20 mg/mL) at the left buccal mucosa of rats on an alternate day for 60 days. OSF: oral submucosa fibrosis; ANE: Areca nut extract



agent for the prevention and treatment of OSF. Further, the same group revealed that EGCG was capable of inhibiting the activation of *TGF- β 1* and connective tissue growth factor (CTGF/CCN2) induced by thrombin in a dose-dependent manner (Liao et al. 2018). However, we have proved that the binding to TGF- β 1 and LOX in in silico models and in vivo proof of concept in rat model of OSF been proved. EGCG was reported for its protect human gingival fibroblasts by its anti-inflammatory properties mainly inhibiting tumour necrosis factor (TNF- α) which is the main mediator of inflammation (Karami et al. 2021). Hence, our study creates new platform for showing the efficacy of developed EGCG formulation.

The EGCG hydrogel was screened in ANE induced rat model of OSF. The areca nut chewing is the cause for oxidative stress and the low antioxidants stimulate the fibroblast to release pro-fibrotic factors to propagate in to OSF. The alkaloid arecoline present in areca nut enhances the collagen

production and reduces its degradation as it activates the fibroblasts and leads to juxtaepithelial inflammatory reaction and disturbs the antioxidant levels followed by OSF generation. The ANE-induced OSF in rats is mimicking the human pathogenesis, where most of the disease markers and oxidative stress were elevated. The main markers such as mouth opening test and body weight changes were almost similar to human OSF (Maria et al. 2016; Shekatkar et al. 2022). EGCG hydrogel showed an improvement in the antioxidant level compared to the OSF-induced rats, which was due to the ability of the EGCG hydrogel to suppress the oxidants or free radicals present and improve the antioxidant activity. It also showed improvement in disease condition by significant reduction in the concentration of TGF- β 1 and collagen concentration. In addition, the preparation of mucoadhesive formulation helped in the retention of EGCG at the buccal mucosal membrane and provided longer duration of action (Tran and Tran 2021; Kumar et al.

2022). Even though both EGCG hydrogel and BTM inj. showed an equal improvement in disease condition, EGCG hydrogel can be considered as more potential strategy for the treatment of OSF condition as the topical formulation can be sufficient for treatment without any side effects as the formulation contain non-toxic and plant-based active moiety. The Ayurvedic formulations such as Erandabhrishta Haritaki and Pippalyadi Choorna are reported for traditional use in oral malignancies (Chakravarthy et al. 2020). Curcumin was recently tried in patient with favorable outputs (Rajbhoj et al. 2021). The standard treatment, BTM inj. reported side effects with higher chances of infection at the site of injection, which decreases the treatment efficiency (Srikanth et al. 2017). Thus, EGCG hydrogel can be considered as safer and more effective in OSF rat model which can be further tested in human volunteers. The current study also assists in developing the novel treatment strategy for OSF therapy which can be tried clinically and fastens the recovery process of patient with reduced treatment duration.

Conclusion

In the present study, various polyphenols were screened for the potential use in OSF therapy. The combination of in silico, in vitro and in vivo studies can be the best platform for selection of suitable polyphenol and examination of its efficacy and safety. EGCG and QUR showed higher affinity and stability towards the selected proteins such as TGF- β 1 and LOX in in silico studies. Additionally, EGCG was effective and safer at higher concentration and helped in significant reduction mRNA expression level of *TGF- β 1*, *COL1A2* and *COL3A1* in buccal fibroblast cells. Further the EGCG hydrogel had an ability and potential for reduction of TGF- β 1 and collagen type-1 and mitigated the oxidative stress in OSF induced rat model. Based on these results, the polyphenol EGCG is a promising phyto molecule for OSF therapy which may improve the patient compliance.

Acknowledgements 1. Department of Pharmaceutics, Manipal College of Pharmaceutical Sciences, Manipal, for in silico computational facilities. 2. Manipal Centre for Biotherapeutics Research, Manipal Academy of Higher Education, Manipal, for in vitro study facilities.

Author contributions **CRedit authorship contribution statement.** **Chetan Hasmukh Mehta:** conceptualization, data curation, formal analysis, methodology, validation, visualization, and writing—original draft. **Shivangi Paliwal:** methodology and analysis, **Manjunatha S. Muttigi:** methodology and analysis, **Raviraja N. Seetharam:** resources, supervision, and analysis, **Alevoor Srinivas Bharath Prasad:** methodology, analysis, and writing original draft, **Yogendra Nayak:** supervision, writing—review and editing. **Shruthi Acharya:** resources, supervision, manuscript review and editing. **Usha Yogendra Nayak:** conceptualization, methodology, project administration, resources, supervision, and manuscript review and editing.

Funding Open access funding provided by Manipal Academy of Higher Education, Manipal. DST-SERB, New Delhi, to procure computers for the Schrodinger's Software (EMR/2016/007006) to Dr. Usha Y Nayak; Senior Research Fellowship (ICMR-SRF No. – 45/18/2020-Nano/BMS) to Mr. Chetan Hasmukh Mehta.

Data availability The datasets generated during and/or analysed during the current study are not publicly available due to the major part is unpublished research work in the spreadsheet, once sorted out and archived, but are available from the corresponding author on reasonable request.

Declarations

Conflict of interest The authors declare that they have no known competing financial interests or personal relationships that could have appeared to influence the work reported in this paper.

Ethics approval Institutional ethics committee approval For the buccal mucosal fibroblast culture, buccal mucosal samples were collected after having informed consent from healthy volunteers according to the approved protocol by the Institutional Ethical Committee (IEC), KMC, Manipal (Approval number: 285/2021).

Institutional animal ethics committee approval The experiments were performed as per Committee for the Purpose of Control and Supervision of Experiments on Animals (CPCSEA) guidelines, India. Institutional Animal Ethical Committee (IAEC), Kasturba Medical College, MAHE, Manipal, was obtained before the experiments (# IAEC/KMC/112/2018).

Open Access This article is licensed under a Creative Commons Attribution 4.0 International License, which permits use, sharing, adaptation, distribution and reproduction in any medium or format, as long as you give appropriate credit to the original author(s) and the source, provide a link to the Creative Commons licence, and indicate if changes were made. The images or other third party material in this article are included in the article's Creative Commons licence, unless indicated otherwise in a credit line to the material. If material is not included in the article's Creative Commons licence and your intended use is not permitted by statutory regulation or exceeds the permitted use, you will need to obtain permission directly from the copyright holder. To view a copy of this licence, visit <http://creativecommons.org/licenses/by/4.0/>.

References

- Adtani PN, Narasimhan M, Punnoose AM, Kambalachenu HR (2017) Antifibrotic effect of *Centella asiatica* Linn and Asiatic acid on arecoline-induced fibrosis in human buccal fibroblasts. *J Invest Clin Dent*. <https://doi.org/10.1111/JICD.12208>
- Adtani P, Malathi N, Ranganathan K et al (2018) Antifibrotic effect of *Ocimum basilicum* L. and linalool on arecoline-induced fibrosis in human buccal fibroblasts: an in vitro study. *Transl Res Oral Oncol*. <https://doi.org/10.1177/2057178X18764471>
- Adtani P, Narasimhan M, Ranganathan K et al (2019) Characterization of oral fibroblasts: an in vitro model for oral fibrosis. *J Oral Maxillofac Pathol* 23:198–202. https://doi.org/10.4103/jomfp.JOMFP_28_19
- Ağagündüz D, Şahin TÖ, Yılmaz B et al (2022) Cruciferous vegetables and their bioactive metabolites: from prevention to novel therapies of colorectal cancer. *Evid Based Complement Alternat Med*. <https://doi.org/10.1155/2022/1534083>

- Akkol EK, Genç Y, Karpuz B et al (2020) Coumarins and coumarin-related compounds in pharmacotherapy of cancer. *Cancers (basel)* 12:1959. <https://doi.org/10.3390/CANCERS12071959>
- Akshaya K, Senthil Murugan P (2021) Assessment of incidence of oral submucous fibrosis patients - An institutional study. *Int J Dent Oral Sci* 8:1939–1945. <https://doi.org/10.19070/2377-8075-21000384>
- Banerjee A, Mampilly M, Kamath V et al (2021) Phenotypic expression of oral fibroblasts derived from oral submucous fibrosis: an assay through cell culture. *J Pharm Bioallied Sci* 13:S1234–S1239. https://doi.org/10.4103/jpbs.jpbs_408_21
- Bowers KJ, Chow E, Xu H, et al (2006) Scalable algorithms for molecular dynamics simulations on commodity clusters. *Proc 2006 ACM/IEEE Conf Supercomput SC'06*. doi:<https://doi.org/10.1145/1188455.1188544>
- Chakravarthy PK, Smriti K, Yeturu SK (2020) Role of herbal and natural products in the management of potentially malignant oral disorders. In: *Natural Oral Care in Dental Therapy*. Wiley, pp 61–79
- Chandran KVA, Abhinethra MS, Deepak TA et al (2022) Effectiveness of Omega-3 fatty acids and spirulina as an adjuvant antioxidant to corticosteroid in the treatment of oral submucous fibrosis—a comparative study. *J Indian Acad Oral Med Radiol* 34:150–155. https://doi.org/10.4103/jiaomr.jiaomr_212_21
- Chiang MH, Lee KT, Chen CH et al (2020) Photobiomodulation therapy inhibits oral submucous fibrosis in mice. *Oral Dis* 26:1474–1482. <https://doi.org/10.1111/odi.13409>
- Chow HH, Cai Y, Alberts DS et al (2001) Phase I pharmacokinetic study of tea polyphenols following single-dose administration of epigallocatechin gallate and polyphenon E-PubMed. *Cancer Epidemiol Biomarkers Prev* 10:53–58
- Devarajan H, Somasundaram S (2019) Oral submucous fibrosis: etiology and management—a review. *Drug Invent Today* 11:1392–1395
- El-feky GS, Zayed GM (2019) PLGA Nanoparticles loaded mucoadhesive and thermosensitive hydrogel as a potential platform for the treatment of oral mucositis. *Int J Appl Pharm* 11:106. <https://doi.org/10.22159/ijap.2019v11i1.29466>
- Farooq U, Khan T, Shah SA et al (2021) Isolation, characterization and neuroprotective activity of folecitin: An in vivo study. *Life* 11:825. <https://doi.org/10.3390/LIFE11080825/S1>
- Ferrarini EG, Paes RS, Baldasso GM et al (2022) Broad-spectrum cannabis oil ameliorates reserpine-induced fibromyalgia model in mice. *Biomed Pharmacother* 154:113552. <https://doi.org/10.1016/J.BIOPHA.2022.113552>
- Friesner RA, Banks JL, Murphy RB et al (2004) Glide: a new approach for rapid, accurate docking and scoring. 1. method and assessment of docking accuracy. *J Med Chem* 47:1739–1749. <https://doi.org/10.1021/jm0306430>
- Friesner RA, Murphy RB, Repasky MP et al (2006) Extra precision glide: docking and scoring incorporating a model of hydrophobic enclosure for protein-ligand complexes. *J Med Chem* 49:6177–6196. <https://doi.org/10.1021/jm051256o>
- Gopinath D, Hui LM, Veettil SK et al (2022) Comparative efficacy of interventions for the management of oral submucous fibrosis: a systematic review and network meta-analysis. *J Pers Med* 12(8):1272
- Halgren T (2007) New method for fast and accurate binding-site identification and analysis. *Chem Biol Drug Des* 69:146–148. <https://doi.org/10.1111/j.1747-0285.2007.00483.x>
- Halgren TA (2009) Identifying and characterizing binding sites and assessing druggability. *J Chem Inf Model* 49:377–389. <https://doi.org/10.1021/ci800324m>
- Halgren TA, Murphy RB, Friesner RA et al (2004) Glide: A new approach for rapid, accurate docking and scoring. 2. Enrichment factors in database screening. *J Med Chem* 47:1750–1759. <https://doi.org/10.1021/jm030644s>
- Haque MA, Hossain MS, Sayed NMA et al (2022) *Abelmoschus esculentus* (L.) moench pod extract revealed antagonistic effect against the synergistic antidiabetic activity of metformin and acarbose upon concomitant administration in glucose-induced hyperglycemic mice. *Biologics* 2:128–138. <https://doi.org/10.3390/BIOLOGICS2020010/S1>
- Harder E, Damm W, Maple J et al (2016) OPLS3: A force field providing broad coverage of drug-like small molecules and proteins. *J Chem Theory Comput* 12:281–296. <https://doi.org/10.1021/acs.jctc.5b00864>
- Hira T, Ahmed KO, Tariq AM (2016) Augmentation of oral submucous fibrosis by NSAIDs in the presence of risk factors. *Pak J Pharm Sci* 29:461–465
- Hossain S, Urbi Z, Karuniawati H et al (2021) *Andrographis paniculata* (Burm. f.) Wall. ex nees: an updated review of phytochemistry, antimicrobial pharmacology, and clinical safety and efficacy. *Life (basel, Switzerland)* 11:348. <https://doi.org/10.3390/LIFE11040348>
- Hsieh Y-P, Chen H-M, Lin H-Y et al (2017) Epigallocatechin-3-gallate inhibits transforming-growth-factor- β 1-induced collagen synthesis by suppressing early growth response-1 in human buccal mucosal fibroblasts. *J Formos Med Assoc* 116:107–113. <https://doi.org/10.1016/j.jfma.2016.01.014>
- Hsieh Y-P, Wu K-J, Chen H-M, Deng Y-T (2018) Arecoline activates latent transforming growth factor β 1 via mitochondrial reactive oxygen species in buccal fibroblasts: suppression by epigallocatechin-3-gallate. *J Formos Med Assoc* 117:527–534. <https://doi.org/10.1016/j.jfma.2017.07.003>
- Iqbal J, Abbasi BA, Ahmad R et al (2020) Phytochemical synthesis of Nickel Oxide Nanoparticles (NiO) using fresh leaves extract of *rhamnus triquetra* (Wall.) and investigation of its multiple in vitro biological potentials. *Biomedicines* 8:117. <https://doi.org/10.3390/BIOMEDICINES8050117>
- Jacobson MP, Pincus DL, Rapp CS et al (2004) A hierarchical approach to all-atom protein loop prediction. *Proteins Struct Funct Genet* 55:351–367. <https://doi.org/10.1002/prot.10613>
- Jahan I, Khan MF, Sayeed MA et al (2022) Neuropharmacological and antiarrhythmic potentials of *duabanga grandiflora* (DC.) Walp. stem bark and prospective ligand-receptor interactions of its bioactive lead molecules. *Curr Issues Mol Biol* 44:2335–2349. <https://doi.org/10.3390/CIMB44050159>
- Kamiloglu S, Sari G, Ozdal T, Capanoglu E (2020) Guidelines for cell viability assays. *Food Front* 1:332–349. <https://doi.org/10.1002/FFT2.44>
- Karami E, Esfahrood Z, Mansouri R et al (2021) Effect of epigallocatechin-3-gallate on tumor necrosis factor-alpha production by human gingival fibroblasts stimulated with bacterial lipopolysaccharide: an in vitro study. *J Indian Soc Periodontol* 25:11–16. https://doi.org/10.4103/jisp.jisp_323_20
- Khan MF, Bin KF, Arman M et al (2020) Pharmacological insights and prediction of lead bioactive isolates of Dita bark through experimental and computer-aided mechanism. *Biomed Pharmacother*. <https://doi.org/10.1016/J.BIOPHA.2020.110774>
- Kondaiah P, Pant I, Khan I (2019) Molecular pathways regulated by areca nut in the etiopathogenesis of oral submucous fibrosis. *Periodontol* 80:213–224. <https://doi.org/10.1111/prd.12266>
- Kumar R, Islam T, Nurunnabi M (2022) Mucoadhesive carriers for oral drug delivery. *J Control Release* 351:504–559. <https://doi.org/10.1016/j.jconrel.2022.09.024>
- Küpelı Akkol E, Tahtı Çankaya İ, Şeker Karatoprak G et al (2021) Natural Compounds as Medical Strategies in the Prevention and Treatment of Psychiatric Disorders Seen in Neurological Diseases. *Front Pharmacol* 12:669638. <https://doi.org/10.3389/fphar.2021.669638>
- Li X, Jin Q, Yao Q et al (2018) The flavonoid quercetin ameliorates liver inflammation and fibrosis by regulating hepatic macrophages

- activation and polarization in mice. *Front Pharmacol*. <https://doi.org/10.3389/fphar.2018.00072>
- Liao Y-W, Yu C-C, Hsieh P-L, Chang Y-C (2018) miR-200b ameliorates myofibroblast transdifferentiation in precancerous oral submucous fibrosis through targeting ZEB2. *J Cell Mol Med*. <https://doi.org/10.1111/jcmm.13690>
- Liu Z, Wang Y, Zhu H et al (2018) Matrine blocks AGEs- induced HCSMCs phenotypic conversion via suppressing Dll4-Notch pathway. *Eur J Pharmacol* 835:126–131. <https://doi.org/10.1016/j.ejphar.2018.07.051>
- Madhavi Sastry G, Adzhigirey M, Day T et al (2013) Protein and ligand preparation: parameters, protocols, and influence on virtual screening enrichments. *J Comput Aided Mol Des* 27:221–234. <https://doi.org/10.1007/s10822-013-9644-8>
- Maria S, Kamath VV, Satelur K, Rajkumar K (2016) Evaluation of transforming growth factor beta1 gene in oral submucous fibrosis induced in Sprague-Dawley rats by injections of areca nut and pan masala (commercial areca nut product) extracts. *J Cancer Res Ther* 12:379–385. <https://doi.org/10.4103/0973-1482.148729>
- Mechchate H, Ouedrhiri W, Es-safi I et al (2021) Optimization of a new antihyperglycemic formulation using a mixture of linum usitatissimum L., Coriandrum sativum L., and Olea europaea var. sylvestris flavonoids: a mixture design approach. *Biologics* 1:154–163. <https://doi.org/10.3390/BIOLOGICS1020009>
- Mitra S, Das R, Bin ET et al (2022) Diallyl disulfide: a bioactive garlic compound with anticancer potential. *Front Pharmacol* 13:943967. <https://doi.org/10.3389/FPHAR.2022.943967>
- Rajbhaj AN, Kulkarni TM, Shete A et al (2021) A comparative study to evaluate efficacy of curcumin and aloe vera gel along with oral physiotherapy in the management of oral submucous fibrosis: a randomized clinical trial. *Asian Pacific J Cancer Prev* 22:107–112. <https://doi.org/10.31557/APJCP.2021.22.S1.107>
- Ray JG, Chatterjee R, Chaudhuri K (2019) Oral submucous fibrosis: A global challenge. Rising incidence, risk factors, management, and research priorities. *Periodontol* 2000 80:200–212. <https://doi.org/10.1111/prd.12277>
- Saran G, Umapathy D, Misra N et al (2018) A comparative study to evaluate the efficacy of lycopene and curcumin in oral submucous fibrosis patients: a randomized clinical trial. *Indian J Dent Res* 29:303–312. https://doi.org/10.4103/ijdr.IJDR_551_16
- Sharma A, Kumar R, Johar N, Sabir H (2017) Clinical discussion oral submucous fibrosis: an etiological dilemma. *J Exp Ther Oncol* 12:163–166
- Sharma M, Shetty SS, Radhakrishnan R (2018) Oral submucous fibrosis as an overhealing wound: Implications in malignant transformation. *Recent Pat Anticancer Drug Discov* 13:272–291. <https://doi.org/10.2174/1574892813666180227103147>
- Shekatkar M, Kheur S, Sanap A et al (2022) A novel approach to develop an animal model for oral submucous fibrosis. *Med Oncol*. <https://doi.org/10.1007/s12032-022-01760-6>
- Shih Y-H, Wang T-H, Shieh T-M, Tseng Y-H (2019) Oral submucous fibrosis: A review on etiopathogenesis, diagnosis, and therapy. *Int J Mol Sci*. <https://doi.org/10.3390/ijms20122940>
- Srikanth G, Komal S, Jyotsna R, Kalyana CP (2017) Unusual complication of intralesional corticosteroid in oral submucous fibrosis patient. *Biomed Pharmacol J* 10:1009–1013. <https://doi.org/10.13005/bpj/1198>
- Tran PHL, Tran TTD (2021) Mucoadhesive formulation designs for oral controlled drug release at the colon. *Curr Pharm Des* 27:540–547. <https://doi.org/10.2174/1381612826666200917143816>
- Uddin Chy MN, Adnan M, Chowdhury MR et al (2021) Central and peripheral pain intervention by Ophiorrhizarugosa leaves: Potential underlying mechanisms and insight into the role of pain modulators. *J Ethnopharmacol* 276:114182. <https://doi.org/10.1016/J.JEP.2021.114182>
- Vieira G, Cavalli J, Gonçalves ECD et al (2020) Antidepressant-like effect of terpineol in an inflammatory model of depression: involvement of the cannabinoid system and D2 dopamine receptor. *Biomolecules* 10:792. <https://doi.org/10.3390/BIOM10050792>
- Wollina U, Verma SB, Faridi M, Patil K (2015) Oral submucous fibrosis: an update. *Clin Cosmet Investig Dermatol* 8:193–204. <https://doi.org/10.2147/CCID.S80576>
- Xia L, Li B (2019) Research progress of curcumin in anti-oral submucous fibrosis. *Med J Chinese People's Lib Army* 44:357–360. <https://doi.org/10.11855/j.issn.0577-7402.2019.04.16>
- Zeng H, He Y, Yu Y et al (2018) Resveratrol improves prostate fibrosis during progression of urinary dysfunction in chronic prostatitis by mast cell suppression. *Mol Med Rep* 17:918–924. <https://doi.org/10.3892/mmr.2017.7960>
- Zhang X, Wang Q, Wu J et al (2018) Crystal structure of human lysyl oxidase-like 2 (hLOXL2) in a precursor state. *Proc Natl Acad Sci USA* 115:3828–3833. <https://doi.org/10.2210/PDB5ZE3/PDB>

Publisher's Note Springer Nature remains neutral with regard to jurisdictional claims in published maps and institutional affiliations.

Authors and Affiliations

Chetan Hasmukh Mehta¹ · Shivangi Paliwal² · Manjunatha S. Muttigi² · Raviraja N. Seetharam² · Aleevoor Srinivas Bharath Prasad³ · Yogendra Nayak⁴ · Shruthi Acharya⁵ · Usha Yogendra Nayak¹ 

✉ Usha Yogendra Nayak
usha.nayak@manipal.edu

¹ Department of Pharmaceutics, Manipal College of Pharmaceutical Sciences, Manipal Academy of Higher Education, Manipal 576104, Karnataka, India

² Manipal Centre for Biotherapeutics Research, Manipal Academy of Higher Education, Manipal 576104, Karnataka, India

³ Department of Ageing Research, Manipal School of Life Sciences, Manipal Academy of Higher Education, Manipal 576104, Karnataka, India

⁴ Department of Pharmacology, Manipal College of Pharmaceutical Sciences, Manipal Academy of Higher Education, Manipal 576104, Karnataka, India

⁵ Department of Oral Medicine and Radiology, Manipal College of Dental Sciences, Manipal, Manipal Academy of Higher Education, Manipal 576104, Karnataka, India